Australian Journal of Basic and Applied Sciences, 4(5): 773-778, 2010
ISSN 1991-8178

Finite Element Analysis of RC Beams Strengthened with FRP Sheets under Bending

[1]Reza Mahjoub, [2]Seyed Hamid Hashemi

[1]MSC, Faculty of Engineering, Islamic Azad University, KhoramAbad Branch, Khoramabad, Iran,
[2]Academic Member, Department of Civil Engineering, University of Arak, Arak, Iran,

Abstract: Attaching unidirectional FRP to the tension face of RC beams has provided an increase in stiffness and load capacity of the structure. However, due to the brittle nature of unidirectional FRP, the ductility of the beam decreases. Consequently, the safety of the structure is compromised due to the reduction in ductility. In this paper after the experimental study, three-dimensional nonlinear finite element (FE) models adopted by ANSYS to examine the structural behavior of the reinforced high strength concrete (HSC) beams strengthened with FRP sheets. The major test variables were included the different layouts of CFRP sheets and tensile reinforcement ratio. More particularly, the change in strength of the beams as the number of FRP layers and tensile reinforcement bar ratio are altered is investigated. Six under-reinforced concrete beams were fabricated and tested to failure. With the exception of the control beam, one or four layers of CFRP were applied to the specimens. The crack patterns in the beams are also presented. The load deflection plots obtained from numerical study show good agreement with the experimental results.

Key words: Finite Element Model, FRP, High Strength Concrete, Ultimate Strength.

INTRODUCTION

The high strength-to-weight ratio, resistance to electro-chemical corrosion, larger creep strain, good fatigue strength, potential for decreased installation costs and repairs due to lower weight in comparison with steel, and nonmagnetic and non-metallic properties of fibre reinforced polymer (FRP) composites offer a viable alternative to bonding of steel plates. The emergence of high strength epoxies has also enhanced the feasibility of using CFRP sheets and carbon fibre fabric for repair and rehabilitation. The failure modes of concrete beams retrofitted with FRP materials and the techniques used in analyzing the failure modes were reviewed by Toutanji *et al.* (2006). The behavior of concrete beams strengthened with externally bonded steel plates (Oh *et al.,* 2003), FRP plates (Chahrour and Soudki, 2005), carbon fibre fabric (Alagusundaramoorthy *et al.,* 2003) and GFRP sheets (Saadatmanesh and Ehsani, 1991) was studied both experimentally and analytically. Malek *et al.* (1998) presented analytical and Hashemi *et al.* (2007) presented numerical finite element procedures to calculate the flexural strength of RC beams bonded with FRP plates. To date, extensive research work has been conducted on the flexural strength of concrete beams bonded with various types of FRP composites.

The objective of this investigation is to study the effectiveness of FRP sheets on ductility and flexural strength of reinforced high strength concrete (HSC) beams. This objective is achieved by conducting the following tasks: (1) flexural testing of reinforced HSC beams strengthened with different amounts of cross-ply of FRP sheets with different amount of tensile reinforcement; (2) calculating the effect of different layouts of FRP sheets on the flexural strength; (3) evaluating the failure modes and (4) three-dimensional nonlinear finite element models are developed to examine the test beams behavior.

Hsrc Laboratory Beam Specimens:

Beam Detail, Instrumentation and Test Procedure:

Four-point bending flexural tests were conducted up to failure on two HSRC control beams and four HSRC beams strengthened with externally bonded FRP sheets on the tension face. The length, width, and depth (L′b′h) of all beams were kept as 3000′150′250 mm. Each concrete beam was reinforced with two 16-mm diameter for A series and two 22-mm diameter for B series steel bars for tension and two 10-mm-diameter steel bars for compression along with 10-mm-diameter bars at a spacing of 90 mm center-to-center for shear reinforcement. The spacing of stirrups and maximum and minimum reinforcement ratios are in accordance with the provision of the American Concrete Institute (ACI).

Corresponding Author: Reza Mahjoub, MSC, Faculty of Engineering, Islamic Azad University, KhoramAbad Branch, Khoramabad, Iran,
E-mail: r_mahjoob@yahoo.com

Electrical resistance disposable strain gauges, manufactured by TML Measurements Group (Japan), were pasted on the CFRP sheets and on internal reinforcing bars at different locations. The demec and electrical gauges were also attached along the height of beams to measure the concrete strains; these values can be used to find out the strain distribution and the moving neutral axis depth of the beams tested. All beams were loaded in four-point bending to failure with a clear span of 2.7 m, and loading points were located at 450 mm on either side of the mid-span location. The load was applied step-by-step up to failure in a load control manner of test beams. During the test, the strains on steel and concrete, and vertical deflections were measured using LVDTs. The strain gauges, LVDTs, and the load cell were connected through a data acquisition system to a computer and the data was recorded and stored in the computer (Fig. 1).

The main test variables considered in the present study include the FRP sheet layers and tensile bars. The FRP sheet layers varies from 0 to 4 and the bar reinforcement ratio varies from 1.2% to 2.4%. Of the six beams tested, two were set aside as control beams and were not strengthened (AH0, BH0), two beam were strengthened with one layer of CFRP (AH1, BH1) and two beam strengthened with four layer of CFRP (AH4, BH4) where the width of CFRP was 150 mm. For all beams, the shear-span-to-depth ratios are 4.18 and the length of the bonded plate is 2600 mm, which covers almost the full-span length between the supports of the beams. The reason for the full-span-length strengthening with FRP plates is to maximize the strengthening effects by delaying the FRP separation.

Material Properties:

The concrete in the beams was designed for a mean 28-day cube strength of about 100 MPa. For each beam three 100mm′100mm′100mm concrete cube specimens were made at the time of casting and were kept with the beams during curing. The average 28-day concrete cube strength (f_{cu}) was 96.2 MPa. The relationship of cylinder strength (f'_c) and cube strength assumed as (f'_c=0.8 f_{cu}) and thus the average compressive strength (f'_c) was 77 MPa. The measured yield and maximum tensile strength of the 10 and 16 mm rebar was 420.6, 634.1 and 412.5,626.4 MPa respectively. The density and thickness of the CFRP material was 1.78± 0.1 gr/cm^3 and 0.045 mm respectively and 2600 mm long. The Young's modulus (E_{fu}), ultimate tensile stress (f_{fu}) and elongation (e_{fu}) of the FRP sheets were 230 GPa, 3850 MPa and 1.7 ± 0.1 % respectively. FRP sheets externally bonded to the tension face of the concrete beams using a two-component structural epoxy named EP-TX at 1:1 ratio for the first layer and a two-part epoxy named EP-IN at 1:1 ratio for the next layer(s) of FRP. Strengthened concrete beams were cured for at least seven days at room temperature before testing.

Finite Element Analysis Approach:

Nonlinear FE analysis is performed using ANSYS (2003), a general purpose finite element program. This section introduces the elements chosen from the software library and the analytical approach and assumptions used in the analysis. The SOLID65 ANSYS (2003), three-dimensional (3D) reinforced concrete solid element, is used to represent concrete in the models. This element is capable of cracking in tension and crushing in compression, although during this study, it was found that when the crushing capability of the concrete is turned on, the finite element beam models fail prematurely. In addition to the rebar capability of the element, the reinforcing steel can be modelled in ANSYS using a series of two node link (truss) elements, called LINK8, which has three degrees of freedom, translations in the nodal *x*, *y*, and *z* directions, and which is also capable of plastic deformation. Unlike concrete, steel is very uniform and as such generally the specification of a single stress-strain relation is adequate to define it numerically. The SOLID46, 3D layered structural solid element, is used to represent the FRP materials. The element has eight nodes with three translational DOFs at each node. Assuming perfect interlaminate bond, no slippage is allowed between the element layers. The FRP laminates are considered brittle and the stress–strain relationship is roughly linear up to failure (Hashemi *et al.,* 2007; Chansawat *et al.,* 2006).

Comparison Between Experimental Data and Numerical Results:

Load- Displacement Curves:

In this section, the numerical results for all specimens are presented and compared with experimental values. Figures 2 and 3 contain a comparison between the load-displacement curves predicted by ANSYS and the test results for all specimens. As is seen, the agreement is reasonable. The results of ANSYS match the plain specimen better than the strengthened specimens. This may be a result of bond slip between FRP and concrete that is ignored in the current analysis.

In general, the strengthened beams were stiffer and less ductile than the control specimens with a higher ultimate load. As a result compared to a beam reinforced heavily with steel only, beams reinforced with both steel and CFRP have adequate deformation capacity, in spite of their brittle mode of failure.

Failure Pattern:

The cracking patterns and failure for various test beams are shown in Fig. 4. The control beams without strengthening plates was designed to fail in flexure. For the control beams (AH0, BH0), failure was by crushing of the concrete in the compression zone after tension steel yield.

All of the strengthened test beams exhibited the rupture of FRP sheets and failed in the same manner. We attended to the failure of a concrete cover along the tensile reinforcement. The concrete was not initially pre-cracked and the development of the cracks during the reinforcement test is highly influenced by the number of CFRP layer. The occurrence of first crack was delayed and more diffuse. Shear cracks occurred in the shear span length of the beams for an applied load between 70% to 80% of the ultimate load. Finally the sudden propagation of horizontal cracks in the concrete-steel bond region occurs. This type of cracks runs along the weakest surface, which is the concrete-steel interface. It leads to the failure of the beam as soon as the cracks opened and separates the concrete cover from the rest of the beam. It is interesting to note that the weakest point of the assemblage concrete-bond-composite material is not the concrete-composite interface but the concrete-internal steel interface.

From the experimental observation, it can be seen that the bond between FRP and concrete is strong enough to ensure the rupture of the composites, thus when four or less than four layers of carbon fibre are applied, the bond problem is not the controlling factor for failure, thus the force in FRP will reach its ultimate tensile capacity when the beam fails and merge the concrete node with the FRP node in finite element model is a true assumption.

The tension steel in control beams AH0 and BH0 reached its yield strength before the compressive strain in concrete reached 0.003 and the beams failed by crushing of concrete. Even though the control beams failed by crushing of concrete, since the failure was initiated by yielding of tension steel, the mode of failure was mentioned to be under reinforced tension failure thus the behavior of the two control beams was a ductile flexural response. For control beams after the first visible cracks observed, the cracking became extensive and crack widths increased steadily. The shape of the load deflection curves indicates a loss of stiffness at a load of approximately 64 kN for AH0 and 122 KN for BH0. This was due to yielding of the tensile reinforcement and occurred at a mid-span deflection of 21 mm for AH0 and 13.3 mm for BH0. After this point, large flexural cracks opened during the test and eventual ultimate collapse were by concrete crushing within the compression zone, a photograph of which is presented in Fig. 5. The ultimate loads recorded were 81.25 and 149.5 kN for AH0 and BH0, respectively.

In this study, for AH1, AH4, BH1 and BH4 the bond problem is not the controlling factor for failure, thus the force in CFRP will reach its ultimate tensile capacity when the beam fails and the failure mode of the strengthened beams are CFRP rupture in the constant moment region. Fig. 6 shows such a typical failure mode.

Discussions on Flexural Behavior:

Table 1 shows a summary of the flexural behavior of all test beams in terms of flexural loading capacity and deflection. The results are clearly demonstrated the accepted beneficial effects of CFRP layers with regard to stiffening and strengthening of the beams.

Table 1 shows the increase of peak load according to the various strengthening layers of CFRP. The rates of increase of peak loads varied from 1 to 44% for experimental data and 11 to 53% for numerical results depending upon the strengthening method. As the amount of steel reinforcement increases, the additional strength provided by the carbon FRP external reinforcement decreases. The same amount of CFRP reinforcement more than 44% the flexural strength of a lightly reinforced beam (r=1.2%), but only increased by 11.7% the strength of a moderately reinforced beam (r=2.4%).

Load-Strain Response at Mid-span:

The relationship between concrete, CFRP and tensile bar steel strains (measured at mid-span) and applied moment for AH4 and BH4 beams measured from experimental study are plotted in Fig. 7.

Fig. 7 indicates that each curve consists of almost three straight lines with different slopes. The first turning point, A, indicates the cracking of concrete in tension zone. The second turning point, B, refers to the yielding tension steel. The yielding and maximum load (ultimate load) can be found for each beam from its load – strain curve.

For beams AH4 and BH4, the tensile steel and CFRP strains are essentially the same at loads below cracking of the concrete. After cracking, the strains in steel exceeded those of the CFRP laminate. As the load approached the yielding load for the strengthened beam, the strains in steel increased more rapidly than those in the CFRP. This is because the CFRP had begun to debond from the concrete surface nearby cracks. It was noted that the tensile steels strains were always higher than the CFRP strains.

Table 1: Numerical and Experimental Mid-span Deflection and load in Yield and Ultimate Stage of RC Beams Strengthened with CFRP Sheets

		Yield stage				Ultimate stage			
Source	Test beam	Load $P_y(kN)$	Increase over control (%)	$\delta_y(mm)$	Decrease over control (%)	Load $P_u(kN)$	Increase over control (%)	$\delta_u(mm)$	Decrease over control (%)
Experimental	AH0	63.93	---	21	---	81.25	---	102	---
	AH1	69.5	8.7	13	38	89.9	11	50.42	51
	AH4	64.7	1.2	9.83	53.2	117.3	44.4	32.85	67.8
Numerical	AH0	69.2	---	13.5	---	75.4	---	94.3	---
	AH1	72.6	4.9	12.8	5.2	90.2	19.6	40.25	57.4
	AH4	75.7	9.4	12.1	10.4	115.4	53.05	36.4	61.4
Experimental	BH0	122.2	---	13.325	---	149.52	---	95.7	---
	BH1	130	6.4	14.11	-5.9	150	0.5	63.24	33.9
	BH4	118	-3.4	12.86	3.6	167	11.7	30.92	67.7
Numerical	BH0	129.9	---	10.8	---	140.2	---	68.9	---
	BH1	134.8	3.7	10.2	5.6	155.6	10.9	35.4	48.7
	BH4	139.2	7.1	9.8	9.1	172.3	22.9	29.5	57.2

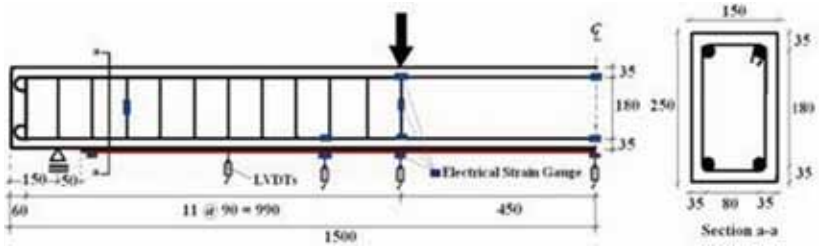

Fig. 1: Beam Details and Measurement Schemes for Half of the Test Specimen (unit: mm)

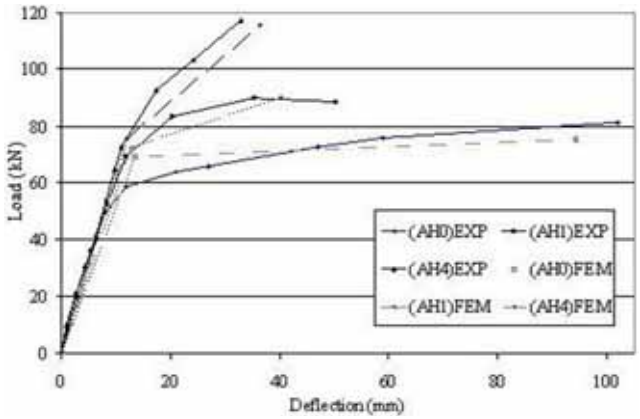

Fig. 2: Load-Displacement Curves Predicted by ANSYS and the Test Result for the A Group Fig. 3: Load-Displacement Curves Predicted by ANSYS and the Test Result for the B Group

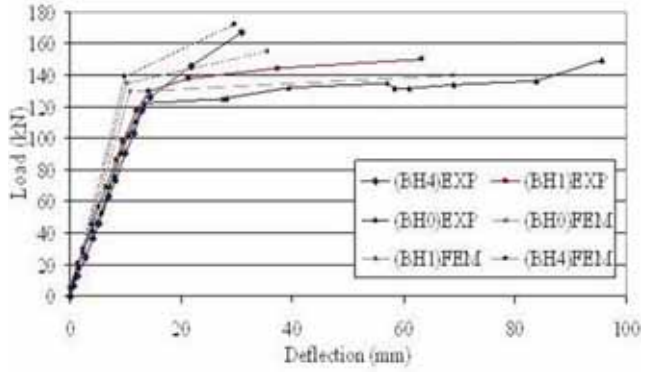

Fig. 3: Load-Displacement Curves Predicted by ANSYS and the Test Result for the B Group

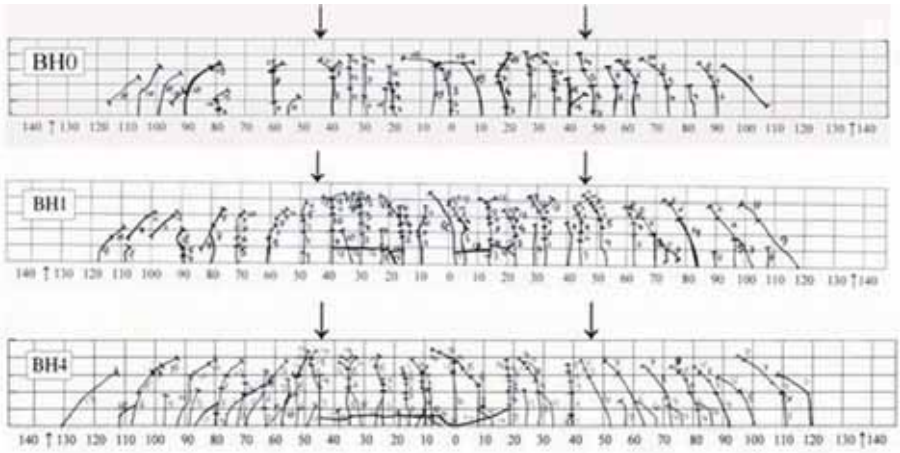

Fig. 4: Failure Configuration of Control and FRP Beams at Ultimate State

Fig. 5: Flexural Failure of Control Beam AH0

Fig. 6: Rupture of FRP in Beam BH4

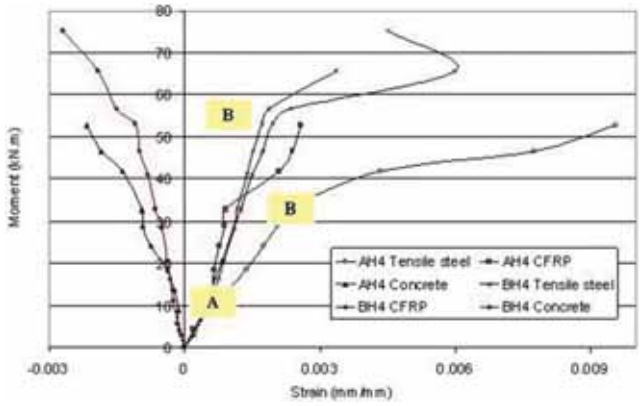

Fig. 7: Moment–Strain Curves of CFRP, Tensile Steel and Extreme Top Concrete Fibre for Beam AH4 and BH4 at Mid-Span

***Conclusions*:**

- The major conclusions derived from this study are given as follows:
- The finite element model results show good agreement with observations and data from the experimental full-scale beam tests. This numerical study can be used to predict the behavior of reinforced concrete beam strengthened with FRP more precisely by assigning appropriate material properties to develop design rules for strengthening RC member using FRP.
- The results of tests performed in this study indicate that significant increase in the flexural strength can be achieved by bonding CFRP sheets to the tension face of high strength reinforced concrete beams. The gain in the ultimate flexural strength was more significant in beams with lower steel reinforcement ratios.
- It was found that for all strengthened test beams, the tensile steels strains were always higher than the CFRP strains.
- The extreme compressive strain of concrete fibre in the strengthened beams with the increased the number of CFRP layers, remains more or less linear up to failure of the beam and is not significantly affected by concrete cracking or yielding of the tension steel. These results demonstrate that the effect of the strengthening plate is to reduce strain in the compression fibres of the concrete.
- Compared to a beam reinforced heavily with steel only, beams reinforced with both steel and CFRP have adequate deformation capacity, in spite of their brittle mode of failure.
- As the amount of tensile steel reinforcement increases, the additional strength provided by the carbon FRP external reinforcement decreases.

REFERENCES

Alagusundaramoorthy, P., I.E. Harik and C.C. Choo, “Flexural Behavior of R/C Beams Strengthened with Carbon Fiber Reinforced Polymer Sheets or Fabric”, Journal of Composites for Construction, 7(4): 292-301.

ANSYS, I., 2003, “ANSYS Manual Set.” ANSYS Inc., Canonsburg, PA 15317, USA.Chansawat, K., Yim, S. and Miller, T., "Nonlinear FE Analysis of a FRP Strengthened Reinforced Concrete Bridge", Journal of Bridge Engineering, 11(1): 21-32.

Chahrour, A. and K. Soudki, 2005. “Flexural Response of Reinforced Concrete Beams Strengthened with End-Anchored Partially Bonded Carbon Fiber-Reinforced Polymer Strips”, Journal of Composites for Construction, 9(2): 170-177.

Hashemi, S.H., R. Rahgozar and A.A. Maghsoudi, 2007. “Finite Element and Experimental Serviceability Analysis of HSC Beams Strengthened with FRP Sheets”, American Journal of Applied Sciences, AJAS, 4(9): 725-735.

Malek, A.M., H. Saadatmanesh and M.R. Ehsani, 1998. “Prediction of Failure Load of R/C Beams Strengthened with FRP Plate Due to Stress Concentration at the Plate End”, ACI Structural Journal, 95(2): 142-152.

Oh, B.H., J.Y. Cho and D.G. Park, “Static and Fatigue Behavior of Reinforced Concrete Beams Strengthened with Steel Plates for Flexure”, Journal of Structural Engineering, 129(4): 527-535.

Saadatmanesh, H. and M.R. Ehsani, 1991. “RC Beams Strengthened with GFRP Plates, I: Experimental Study”, Journal of Structural Engineering, 117(11): 3417-3433.

Toutanji, H., L. Zhao and E. Anselm, 2006. “Verifications of Design Equations of Beams Externally Strengthened with FRP Composites”, Journal of Composites for Construction, 10(3): 254-264.